LANGMUIR
Cite This: Langmuir XXXX, XXX, XXX−XXX
Invited Feature Article
pubs.acs.org/Langmuir

Interfacial Emulsification: An Emerging Monodisperse Droplet Generation Method for Microreactors and Bioanalysis

Shenglong Liao,[†] Yi Tao,[‡,§] Wenbin Du,*[,‡,§] and Yapei Wang*[,†]

[†]Department of Chemistry, Renmin University of China, Beijing 100872, China
[‡]State Key Laboratory of Microbial Resources, Institute of Microbiology, Chinese Academy of Sciences, Beijing 100101, China
[§]Savaid Medical School, University of the Chinese Academy of Sciences, Beijing 100049, China

ABSTRACT: The generation of uniform droplets has been extensively investigated owing to its profound potentials both in scientific research and engineering applications. Although various methods have been put forward to expand this area, new innovations are still needed to improve the technical convenience and save instrumental cost. In this feature article, we highlight an interfacial emulsification technique that we developed in the past several years. This technique serves as a platform for preparing uniform droplets that are formed on the air-liquid interface of the continuous phase based on interfacial shearing. Three specific aspects of interfacial emulsification are reviewed, including its basic design and principle, the preparation of droplets with controllable size and adjustable components, and practical applications of the method in bioanalysis, microreactors, and particle synthesis. Compared to other droplet generation methods, several attractive advantages and perspectives for further development have been summarized.

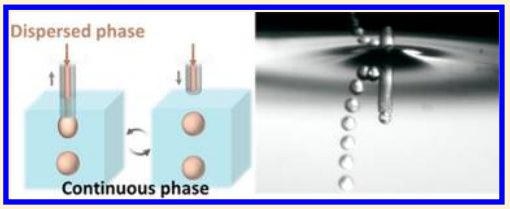

1. INTRODUCTION

The generation of monodisperse droplets is a profound and valuable theme that has attracted numerous interests for more than half a century. In 1950s, the generation of small and uniform droplets was an effective method for the study of sprays of plant-growth regulators, fungicides, and insecticides on leaves.[1] Recently, monodisperse droplets have become unreplaceable tools for research on single-cell analysis,[2] cell sorting,[3] and high-throughput reaction screening.[4,5] Hence, various methods for uniform droplet generation have been proposed and developed, including droplet sizer,[1] spinning-disk sprayer,[6,7] membrane emulsification,[8−10] inkjet printing,[11−13] and microfluidics.[14−20] To date, droplet microfluidics has been the most popular and reliable approach for preparing monodisperse droplets with size ranging from micrometers to millimeters. Compared to traditional methods, droplet microfluidics exhibits great advantages in the generation, manipulation, and analysis of femtoliter to nanoliter droplets. However, droplet microfluidics is still faced with several inherent problems that severely limit its widespread applications: (1) Except for the fact that glass capillary microfluidics exhibits excellent compatibility with different solvents, most microfluidic chips made of elastomeric polymers present poor compatibility with various kinds of organic solvents,[21−23] which hinders their application in chemical synthesis and reaction screening. (2) Designing and fabricating microfluidic devices require skilled technicians and specialized equipment, which restrict their application in laboratories without related facilities.[24,25] (3) Precise control and prediction of droplet size are relatively complicated since the droplet size is affected by many factors that cannot be directly determined. These factors have to be experimentally measured and empirically adjusted. For example, the size and uniformity of droplets are affected by the viscosity of fluids, the interfacial tension and dynamics between immiscible fluids, and the size and structure of microfabricated channels.[26]

To address the rising demands on simple, low-cost, facile methods for monodisperse droplet generation, we developed a novel technique using the shearing force of the air-liquid interface to produce monodisperse droplets, which exhibits several attractive advantages, including high controllability, solvent compatibility, flexibility, inexpensive, easy assembly, and broad availability. Previously, on the basis of the difference in applications, we have termed this technique cross-interface emulsification[27,28] (XiE, for water-in-oil droplets) or dynamic interfacial printing[29,30] (DIP, for particle synthesis). In this feature article, we unify two terms as interfacial emulsification and introduce it from three aspects, including the basic design and principle, precise control of droplet volume and the influence factors, and its applications in microreactors and bioanalysis.

2. BASIC PRINCIPLE OF INTERFACIAL EMULSIFICATION

2.1. Basic Design of Interfacial Emulsification. The basic setup of interfacial emulsification contains three parts: a liquid dispenser, a mechanical vibrator, and a reservoir preloaded with the continuous phase (Figure 1a). Briefly, the syringe pump drives the flow of the dispersed phase from the syringe to the nozzle of the capillary via Teflon tubing. The

Received: April 2, 2018
Revised: May 23, 2018
Published: May 24, 2018

DOI: 10.1021/acs.langmuir.8b01067
Langmuir XXXX, XXX, XXX−XXX

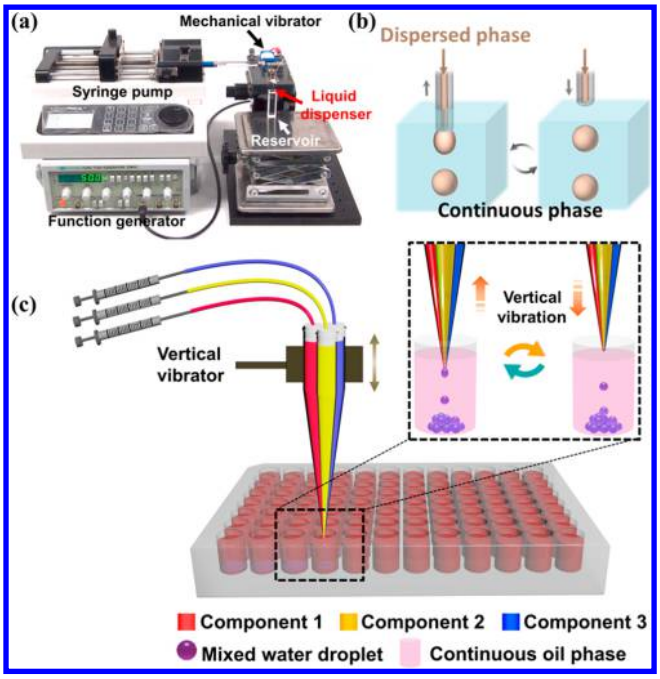

Figure 1. Basic principle of interfacial emulsification. (a) Device setup and (b) schematic illustration of interfacial emulsification.[29] Reprinted with permission from ref 29. Copyright 2016 John Wiley & Sons. (c) Schematic for the generation of multicomponent droplets.[30] Reprinted with permission from ref 30. Copyright 2017 American Chemical Society.

capillary nozzle, which is anchored vertically on the mechanical vibrator, vibrates periodically across the surface of a continuous phase preloaded in the reservoir. Monodisperse droplets are generated at the nozzle and then detach from it once the nozzle lifts away from the surface of the continuous phase. The newly generated droplets are stabilized by surfactants dissolved in the continuous phase. Since the flow is steady and the vibrational process is highly repeatable, droplets generated in each period share the same size in principle, and one droplet is generated during each vibrational cycle. Besides water-in-oil droplets,[23] the interfacial emulsification technique can also generate oil-in-water droplets[25] simply by reversing the dispersed phase and the continuous phase.

To push forward versatile applications of interfacial emulsification, a multichannel glass capillary was introduced for the generation of multicomponent droplets (Figure 1c).[30] Multiple components can be injected through the vibrating nozzle to obtain droplets with precise control of the mixing ratio with the same interfacial shearing mechanism. This method allows the generation of monodisperse droplets with both controllable size and tunable components.

The methodology of interfacial emulsification affords several outstanding advantages in comparison to popular droplet microfluidics. Previous droplet microfluidics commonly relies on microfluidic chips or well-aligned coaxial capillaries, both of which are not easy to achieve or assemble for people without access to microfabrication facilities. On the contrary, the interfacial emulsification can be set up using simple and low-cost parts that can be modularly assembled in several minutes without a tedious microfabrication process. Moreover, the whole fluidic channel (syringe, Teflon tubing, and silica or glass capillary) in interfacial emulsification is highly compatible with various kinds of aqueous or organic solutions, which is a critical challenge for elastomer-based microfluidic chips. The above advantages of interfacial emulsification ensure that this versatile technique can be widely available for many interdisciplinary laboratories.

2.2. Physical Principles of Interfacial Emulsification. As shortly mentioned above, droplet generation relies on the interfacial shearing process. In each vibrational period, only one droplet is produced which has been proven via slow-motion photograph recorded by a high-speed camera. As shown in Figure 2a, during the vibrational period, a pendant aqueous

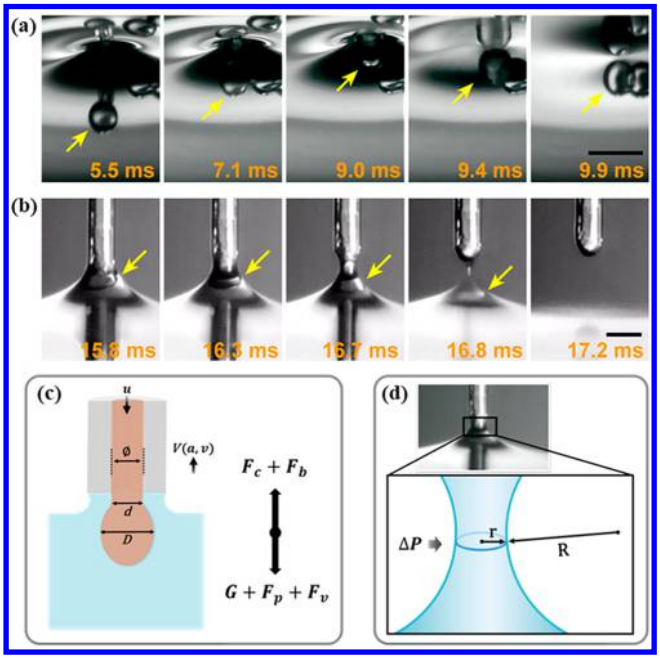

Figure 2. Basic principle of interfacial emulsification. (a, b) Series of slow-motion photographs in one vibrational period captured by a high-speed camera. The droplet phase is the aqueous solution, and the continuous phase is mineral oil with surfactants.[27] Reprinted with permission from ref 27. Copyright 2016 American Chemical Society. (c) Force analysis of the pendant drop moving beneath the continuous phase.[29] (d) Optical photograph captured on a high-speed camera at a frame speed of 6000 fps and the Laplace pressure analysis based on the interfacial curvature.[29] Reprinted with permission from ref 29. Copyright 2016 John Wiley & Sons.

drop hung on the capillary moves beneath the surface of the continuous phase (mineral oil) and spontaneously detaches from the capillary nozzle when the nozzle is rising above the air−liquid interface. On the basis of this phenomenon, a quantitative mathematical model based on a typical interfacial emulsification process is built and divided into two key issues.

The first issue is that the capillary force is large enough to pull the pendant drop in the whole motion process in the continuous phase. As shown in Figure 2c, in the simple harmonic motion process, the pendant drop receives five forces including gravity (G), buoyance force (F_b), capillary force (F_c), injection pressure force (F_p), and the Stoke's drag force (F_v). According to the Newton's second law, the total force equals mass multiplied by acceleration. Thus, the capillary force needs to support the simple harmonic motion of the pendant drop and can be calculated according to eq 1.

$$F_c = F_v + G + F_p + ma - F_b \quad (1)$$

DOI: 10.1021/acs.langmuir.8b01067
Langmuir XXXX, XXX, XXX−XXX

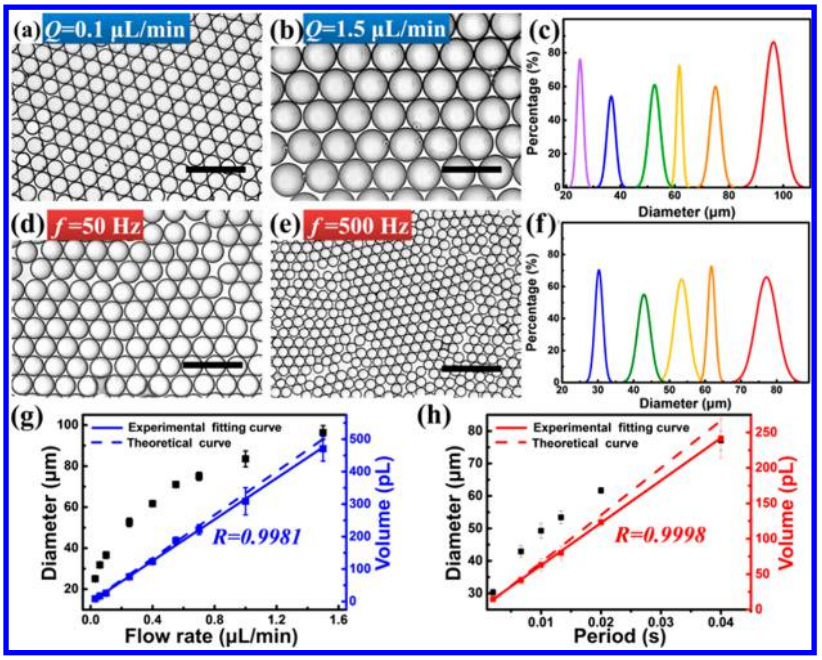

Figure 3. Controllable droplet size in interfacial emulsification by tuning the flow rate and vibrational frequency.[29] (a, b) Bright-field microscopy images of CCl_4 droplets generated at a vibrational frequency of 50 Hz and flow rates of (a) 0.10 and (b) 1.50 μL/min. (c) Size distribution curves of droplets generated at different flow rates and the same vibrational frequency of 50 Hz. (Left to right) 0.03, 0.10, 0.25, 0.40, 0.70, and 1.50 μL/min. (d, e) Optical microscopy images of CCl_4 droplets generated at a flow rate of 0.40 μL/min and vibrational frequencies of (d) 50 and (e) 500 Hz. (f) Size distribution curves of droplets generated at different vibrational frequencies and the same flow rate of 0.40 μL/min. (Left to right) 500, 150, 75, 50, and 25 Hz. (g) Relationship between the droplet size as a function of flow rate at a vibrational frequency of 50 Hz. (h) Relationship between the droplet size as a function of vibrational frequency at a flow rate of 0.40 μL/min. The solid lines in (g) and (h) refer to a linear fitting plot of experimental results, and the dashed line is a theoretical curve according to eq 2. Scale bar: 200 μm. Reprinted with permission from ref 29. Copyright 2016 John Wiley & Sons.

By analyzing the droplet positions at different times in several consecutive vibrational periods, the moving equation of the droplet is determined via fitting the data with a standard harmonic motion equation. Then, the velocity and acceleration that directly decide the Stokes' drag force and the total force are also determined according to the moving equation. The maximum capillary force needed to support drop motion is obtained, which is much smaller than the theoretical capillary force provided by the capillary.

The second issue is that the interfacial shearing at the surface of continuous phase dominated droplet formation. To clearly view the shearing process, a series of slow-motion videos were recorded from a viewpoint above the oil surface, indicating that the air−liquid interface is gradually deformed to a saddle shape when the end of the nozzle rises above the horizontal plane (Figure 2b). Because of surface tension, an inward Laplace pressure existing between the air and the continuous phase would compress the necklike connection between the capillary and liquid, thus leading to the interfacial shearing force that breaks the connection between the dispersed phase and the capillary. Therefore, the Laplace pressure dominated by interfacial tension is the key driving force for dynamic interfacial shearing.

3. DETERMINATION OF DROPLET SIZE AND COMPONENTS

3.1. Precise Control of Droplet Volume. The precise control of droplet size is another important issue for a droplet generation technique. For interfacial emulsification, the basic dynamic shearing process has been captured by a high-speed camera, verifying that one droplet would be generated per vibrational cycle. Thus, it is easy to deduce that the droplet volume (V) equals the flow rate (Q) of the dispersed phase divided by the vibrational frequency (f), which can be simply written as eq 2:

$$V = \frac{Q}{f} \tag{2}$$

Therefore, the droplet diameter can be calculated according to eq 3:

$$D = \left(\frac{6Q}{\pi f}\right)^{1/3} \tag{3}$$

To verify the above deduction, droplets were generated at different flow rates and vibrational frequencies. When the frequency is fixed, droplet diameters at different flow rates exhibit narrow distributions with a coefficient of variation of less than 5%. Similarly, by keeping the same flow rate and changing the vibrational frequency, we can also generate uniform droplets with narrow distributions (Figure 3d−f). According to the statistical data presented in Figure 3g,h, the droplet volume is proportional to the flow rate or the vibrational period, perfectly matching the theoretical curves predicted by eq 2. Thus, it is conclusively demonstrated that droplets with predictable sizes over a wide range can be generated by adjusting the flow rate and the vibrational frequency.

3.2. Control of Multicomponent Droplets Using Interfacial Emulsification. The interfacial emulsification technique can also produce monodisperse multicomponent droplets (Figure 4a−c). Aqueous solutions from different

DOI: 10.1021/acs.langmuir.8b01067
Langmuir XXXX, XXX, XXX−XXX

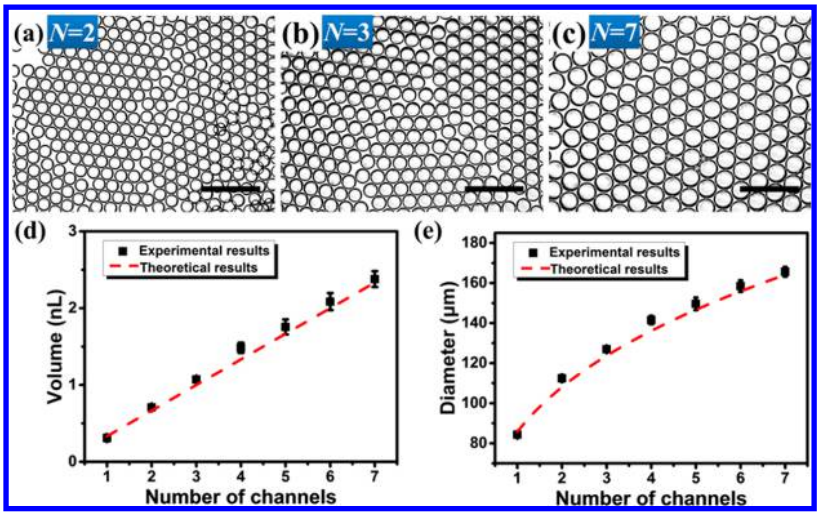

Figure 4. Tuning the size of multicomponent droplets by changing the number of channels with the same flow rate in each channel (1.00 μL/min) and the same vibrational frequency (50 Hz).[30] The droplet phase is the aqueous solution, and the continuous phase is mineral oil. Optical images (a–c) of droplets generated with different numbers of channels. Scale bar: 500 μm. (d, e) Relationship between droplet size and the number of open channels. Droplet volume (d) and droplet diameter (f) versus the number of open channels. Reprinted with permission from ref 30. Copyright 2017 American Chemical Society.

channels converge into a pendant drop at the nozzle tip, and such a pendant drop is subsequently sheared by the air-liquid interface. Thus, the volume and diameter of the droplet generated by interfacial emulsification methods can be calculated by eqs 4 and 5.

$$V = \frac{\sum_{i=1}^{N} Q_i}{f} \tag{4}$$

$$D = \left(\frac{6\sum_{i=1}^{N} Q_i}{\pi f}\right)^{1/3} \tag{5}$$

The above two equations are also verified by experiments upon changing the channel number at the same vibrational frequency and the same flow rate in each channel. The results presented in Figure 4d,e indicate that the droplet volume is proportional to the channel number, which is consistent with the predication.

3.3. Control of Droplet Components in Interfacial Emulsification. Since the droplet volume is proportional to the sum of the flow rates, the concentration of any component ($c_{x,\text{droplet}}$) in a droplet can be easily calculated according to the following linear equation

$$c_{x,\text{droplet}} = \frac{\sum_{i=1}^{N} c_{x,i} Q_i}{\sum_{i=1}^{N} Q_i} \tag{6}$$

where $c_{x,i}$ is the concentration of component in a specific channel. The linear equation has been proven by a quantitative experiment via loading fluorescent dye in droplets. In a typical three-channel capillary, two channels are loaded with the same fluorescein sodium buffer solution (pH 9.18), and the other channel is loaded with the blank buffer solution. Droplets with the same volume generated at different flow rates of two fluorescent channels are shown in Figure 5a–d, and the fluorescence intensities of these droplets are compared. As shown in Figure 5e, the fluorescence intensity exhibits a perfect linear relationship versus the flow rate of the fluorescence channel in the concentration range below 10 μmol/L and

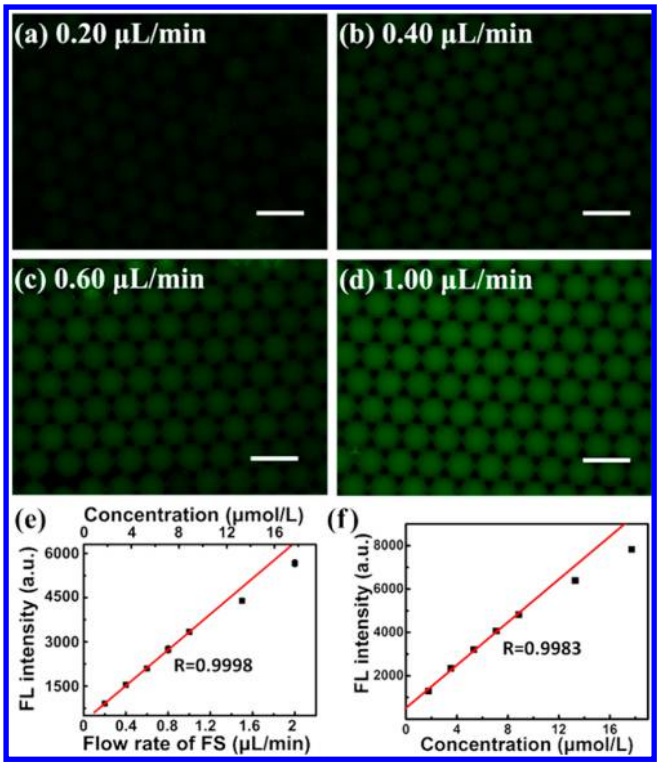

Figure 5. Quantitatively loading fluorescent dye into droplets.[30] (a–d) Fluorescent images of droplets generated at different total flow rates of fluorescein sodium solution. Scale bar: 200 μm. (e) Droplet fluorescence intensities under different total flow rates of fluorescein sodium solution. (f) Fluorescent intensity of the fluorescein sodium solution at different concentrations. Red lines in (e) and (f) are the linear fitting curves of five points at low concentrations. Reprinted with permission from ref 30. Copyright 2017 American Chemical Society.

deviates from the linear line at high concentration due to aggregation-caused quenching. A similar trend is also observed in the bulk solutions as shown in Figure 5f. On the basis of the above results, a conclusion is drawn in which components in droplets generated via interfacial emulsification can be facilely

DOI: 10.1021/acs.langmuir.8b01067
Langmuir XXXX, XXX, XXX–XXX

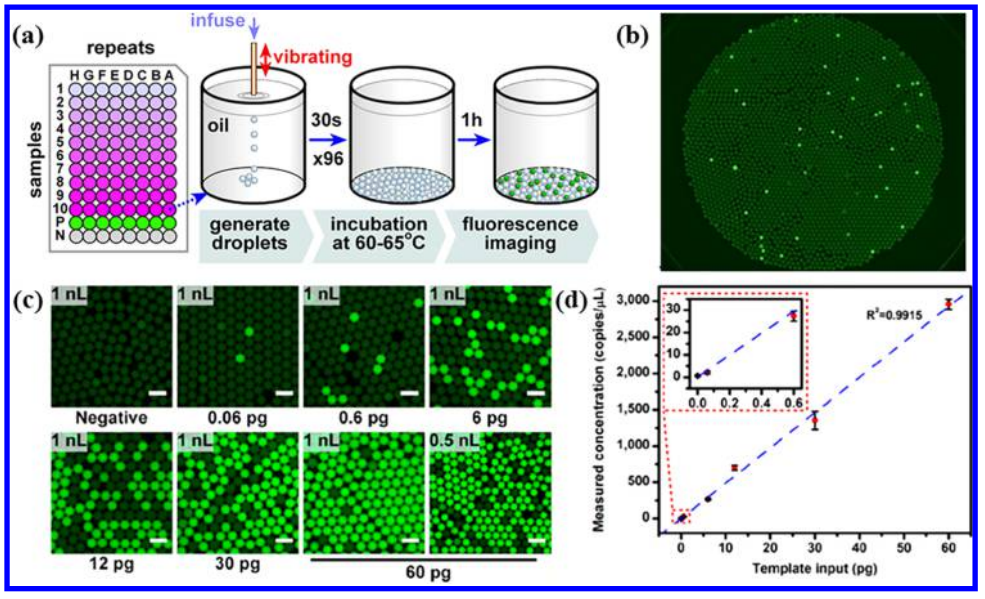

Figure 6. dLAMP based on interfacial emulsification for absolute nucleic acid quantification. (a, b) Brief process of dLAMP, including the generation of droplet arrays in microwells, incubation at 60−65 °C, and fluorescence imaging.[28] Reprinted with permission from ref 28. Copyright 2017 American Chemical Society. (c) Fluorescent images of the PMDAs after the dLAMP reactions. Scale bar: 200 μm.[27] (d) Linear correlation (blue dashed line) between the input and the measured concentration of λ-DNA templates based on dLAMP. The dotted red rectangle shows an expanded view of the correlation at low template concentration.[27] Reprinted with permission from ref 27. Copyright 2016 American Chemical Society.

controlled and predicted, which is of vital importance for microreactors and bioanalysis.

In a brief conclusion, interfacial emulsification could generate highly monodisperse droplets with a narrow size distribution. Additionally, the droplet size and components can be precisely predicted on the basis of the flow rate and the vibrational frequency with a simple calculation. On the contrary, for traditional droplet microfluidic methods including co-flow, flow focusing, and a T-shaped chip, the major size determinant is the geometry of the device (width and depth of the channels). To generate droplets with different sizes, special chip design, fabrication, and surface modification are required. The processes for determining the above factors involve considerable obstacles in droplet size prediction, especially for researchers without relevant facilities or experiences. In comparison, interfacial emulsification can precisely predict droplet size based on a straightforward equation with two simple parameters that can be absolutely defined by users. Moreover, considering that the setup and operation of interfacial emulsification are much easier than traditional droplet microfluidics, the method is bound to be a popular droplet generation technique among researchers from different areas without experience in the fabrication of microfluidic devices.

4. APPLICATIONS OF INTERFACIAL EMULSIFICATION

4.1. Digital Nucleic Acid Amplification for the Absolute Quantification of DNA/RNA. Digital nucleic acid amplification (digital NAA), such as the digital polymerase chain reaction (dPCR)[31−37] and digital loop-mediated isothermal amplification (dLAMP),[38,39] quantifies nucleic acids by confining single DNA or RNA templates in massive tiny compartments and performing parallel amplification. Previously, droplet microfluidic devices were widely adopted in digital NAA, which often relies on sophisticated microfabrication and the precision regulation of flow in multiple channels for both the aqueous phase and the continuous oil phase. In comparison, interfacial emulsification allows more absolute and flexible control of droplet size, which needs only a single pump and requires no microfabricated parts. Moreover, multivolume digital assays[40,41] can be easily realized using interfacial emulsification to provide a wider dynamic range of quantification.

To demonstrate the feasibility of interfacial emulsification for digital NAA, we introduced a simple dLAMP workflow for the quantification of nucleic acid templates in samples (Figure 6a). This workflow can be easily extended to other digital NAA methods. First, we characterize the linearity of dLAMP detection using a series of diluted stock solution of λ-DNA, ranging from 60 fg to 60 pg. Samples were emulsified on a flat-bottomed 96-well plate prefilled with mineral oil. Monodisperse droplets were obtained for each sample in different wells, forming planar monolayer droplet arrays (PMDAs). After incubation at 65 °C for 1 h, PMDA fluorescence imaging was performed using an epifluorescence inverted microscope. Fluorescent images of PMDAs were analyzed to determine the percentage of droplets with high intensity, which is defined as the positive ratio. The concentration of the DNA template was calculated according to the Poisson distribution. The measured template concentration was plotted against the mass of input DNA templates, obtaining a linear fit curve (Figure 6b). Notably, the droplet volume can impose restrictions on the dynamic range of detection of digital NAA since high template concentration will lead to saturation of the positive ratio. For example, when the droplet volume is 1 nL, dLAMP quantification is successfully performed at an input DNA template of less than 60 pg. However, when the input template reaches 60 pg, the dLAMP quantification result (3149 copies/μL) exhibits a severe deviation to the fitting results of lower concentrations. When we adjust the droplet volume to 0.5 nL, the PDMAs have a better resolution for the digital quantification of the 60 pg input DNA, and the result (2955 copies/μL) shows a better linear agreement with lower

DOI: 10.1021/acs.langmuir.8b01067
Langmuir XXXX, XXX, XXX−XXX

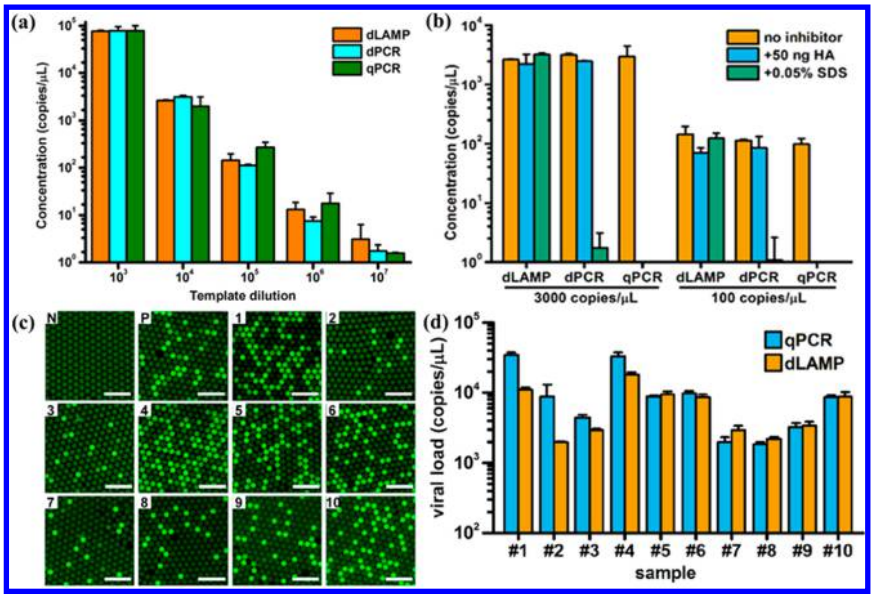

Figure 7. dLAMP based on interfacial emulsification platform for absolute quantification of H5N1 virus.[28] (a) Comparison of dLAMP with qPCR and dPCR in the detection of H5N1 viruses. (b) Quantification of templates by dLAMP, dPCR, and qPCR with and without inhibitors. (c, d) Quantification of H5N1 viral loads in samples harvested from allantoic fluids. (c) Fluorescent images of droplet arrays after the dLAMP reaction for 10 samples with a positive control (P) and a negative control (N). Scale bar: 500 μm. (d) Viral load quantification results by qPCR and dLAMP for all samples. Reprinted with permission from ref 28. Copyright 2017 American Chemical Society.

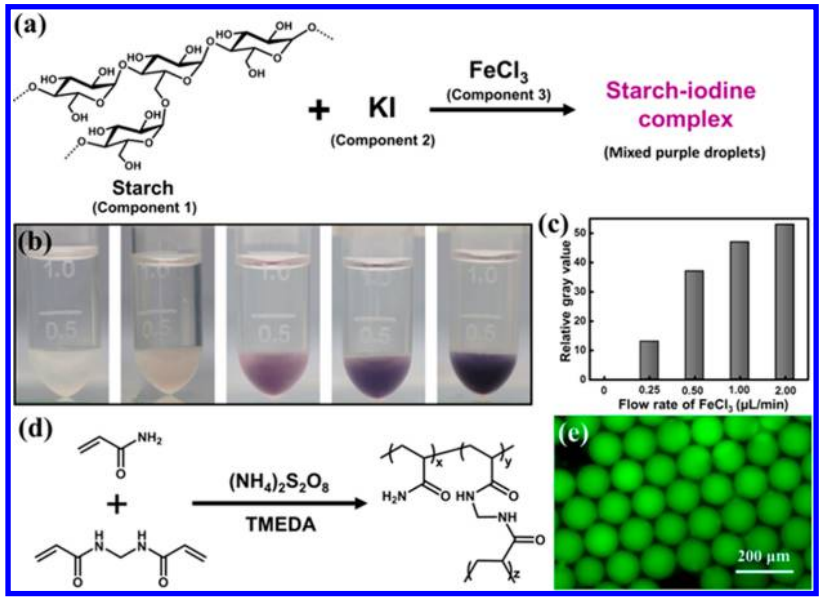

Figure 8. Chemical reactions miniaturized in uniform droplets generated by an interfacial emulsification technique.[30] (a) Three-component chromogenic reaction among starch, potassium iodide, and ferric chloride. (b) Optical images of three-component mixed droplets generated under different flow rates of ferric chloride. (Left to right) 0.00, 0.25, 0.50, 1.00, and 2.00 μL/min. (c) Relative gray value of the droplet region of pictures in (b). (d) Polymerization reaction of acrylamide in droplets. (e) Fluorescent image of polyacrylamide hydrogel microspheres dispersed in petroleum ether without surfactants. Reprinted with permission from ref 30. Copyright 2017 American Chemical Society.

concentrations, which proves the feasibility of multivolume digital NAA using interfacial emulsification.

4.2. Absolute Quantification of the H5N1 Viral Load by dLAMP. The rapid and quantitative detection of highly pathogenic avian influenza (HPAI) is an important issue for infection monitoring and control.[42] Commonly, real-time quantitative PCR (qPCR) is widely accepted as the gold standard in HPAI detection while it relies on expansive equipment and a well-trained operator.[43,44] Recently, dPCR has made a great breakthrough in the absolute quantification of nuclei acid, and integrated commercial instruments have been developed. However, in the dPCR procedure, droplet generation, PCR amplification, and signal collections are performed separately, which may lead to uncontrollable error during the droplet transfer process. Another serious problem for the PCR approach is the poor resistance to some chemical inhibitors that widely exist in soil and fecal samples.

Using the dLAMP workflow built on the basis of interfacial emulsification, we further demonstrated that dLAMP could be utilized in precise viral load tests for H5-subtype HPAI viruses. Typically, prior to measurement, cDNA is synthesized by total virus RNA extraction and reverse transcription. Then, the viral

DOI: 10.1021/acs.langmuir.8b01067
Langmuir XXXX, XXX, XXX−XXX

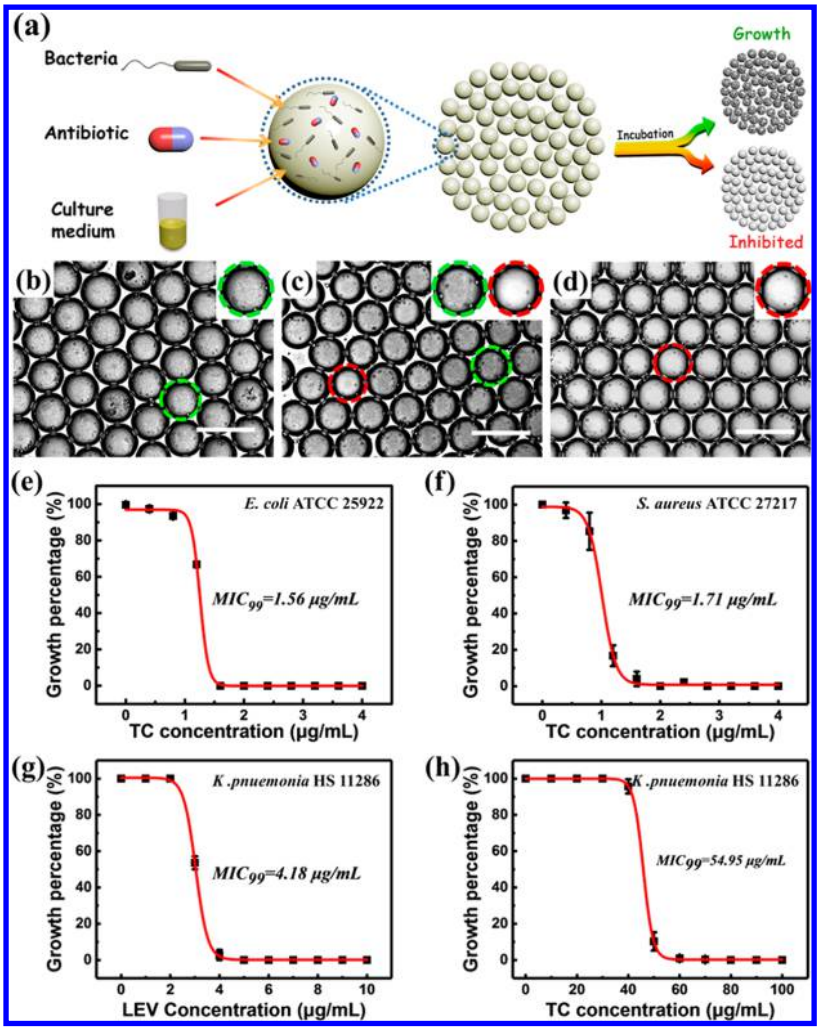

Figure 9. MIC tests using PMDAs generated by interfacial emulsification. (a) Schematic illustration of the three-component droplets for MIC testing.[30] (b–d) Optical images of droplets loaded with *E. coli* ATCC 25922 and different amounts of tetracycline (TC). (b) 0, (c) 0.80, and (d) 2.40 μg/mL. Green dashed circle: droplet with bacterial growth. Red dashed circle: droplet with inhibited bacterial growth. Scale bar: 200 μm. (e, f) Percentage of droplets with bacterial growth versus TC concentration. (e) *E. coli* ATCC 25922. (f) *S. aureus* ATCC 27217. (g, h) Percentage of droplets with bacterial (*K. pneumoniae* HS 11286) growth versus antibiotic concentration. (g) Levofloxacin (LEV). (h) TC. The red curves in (e–h) are the fitting curves of all black points according to the DoseResp model. Reprinted with permission from ref 30. Copyright 2017 American Chemical Society.

loads are calculated by cDNA quantification, which are performed using dLAMP, qPCR, and dPCR in parallel. All three methods yield comparable quantification results for standard 10-fold serially diluted H5 cDNA templates (Figure 7a).

In some cases, the clinical or field-collected samples may contain inhibitory substances that are difficult to remove completely, which impairs quantification by qPCR. To prove the robustness of dLAMP compared to qPCR and dPCR, humic acid (HA) and sodium dodecyl sulfate (SDS) were selected as inhibitors in the viral load tests for H5-subtype HPAI viruses. The results shown in Figure 7b indicate that both HA and SDS at the experimental concentration exhibit no interference with the results of dLAMP. The results of six groups tested via dLAMP are also consistent with the concentration quantified by qPCR and dPCR without inhibitor. In comparison, both HA and SDS cause severe interference and lead to no amplification signal for qPCR. The dPCR performed on a commercial instrument (QX200, Bio-Rad) is not influenced by HA but is significantly inhibited by SDS. As a result, the good tolerance to inhibitors reveals that dLAMP can be potentially utilized to test "dirty" samples. Finally, the dLAMP method is used for the absolute quantification of H5N1 viral loads in 10 allantoic fluid samples. The viral loads tested by dLAMP are consistent with the results of qPCR (Figure 7c,d), indicating that our dLAMP workflow can provide robust and absolute quantification of the viral loads in real samples.

4.3. Multicomponent Microreactors. Owing to the advantages of low sample consumption, rapid reaction, and excellent safety, droplet microreactors have been widely applied as a powerful tool for screening conditions in chemical synthesis.[4,5,45−49] As stated above, interfacial emulsification can generate monodisperse multicomponent droplets precisely with different components and mixing ratios. To demonstrate the practical availability of interfacial emulsification for microreactors, two kinds of model chemical reactions were miniaturized into nanoliter-scale droplets. As presented in Figure 8a, a simple chromogenic reaction among starch, potassium iodide, and ferric chloride is performed in droplets

DOI: 10.1021/acs.langmuir.8b01067
Langmuir XXXX, XXX, XXX−XXX

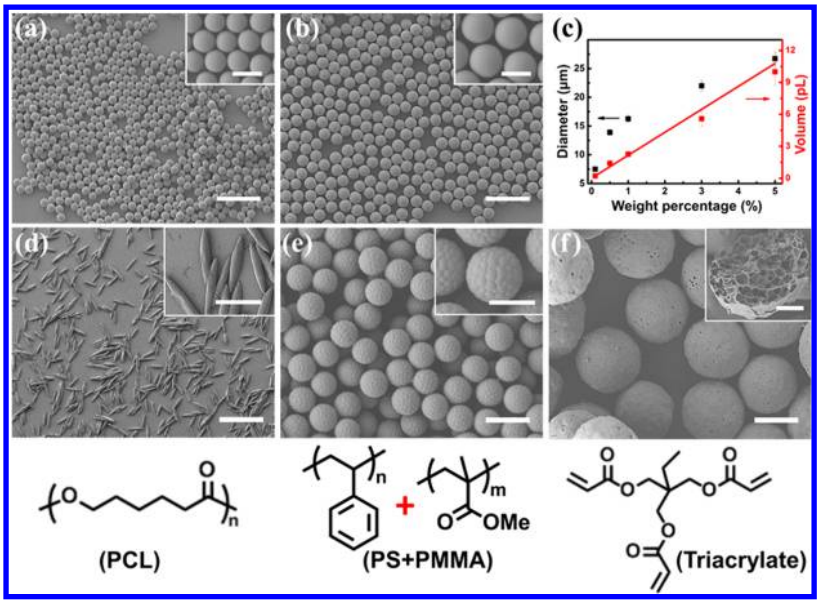

Figure 10. Production of uniform polymeric microparticles via interfacial emulsification.[29] (a, b) SEM images of polystyrene particles solidified from chloroform droplets dissolving polystyrene with different concentrations: (a) 1 and (b) 3 wt %. Scale bar: 100 μm. The scale bars in the insets are 20 μm. (c) Particle size as a function of polystyrene concentration in chloroform. (d) SEM images of elongated polycaprolactone particles with a scale bar of 200 μm and an inset scale bar of 100 μm. (e) SEM images of patchy particles of PS and PMMA blended with a scale bar of 20 μm and an inset scale bar of 10 μm. (f) SEM images of porous particles polymerized by trimethylolpropane triacrylate with a scale bar of 20 μm and an inset scale bar of 10 μm. Reprinted with permission from ref 29. Copyright 2016 John Wiley & Sons.

via the interfacial emulsification technique. The newly generated droplets consisting of the above three components quickly turn purple. The droplet color becomes deeper as the flow rate of ferric chloride increases (Figure 8b,c). The other model microreactor in droplets is the polymerization of acrylamide. As shown in Figure 8d, monomer, cross-linker, and initiator were loaded into the droplets, and the emulsion droplets were surrounded with oil-soluble surfactants to avoid droplet coalescence. About 10 min later, petroleum ether was used to remove the surfactants in the oil phase three times. Interestingly, although the surfactants are removed, the droplets do not coalesce with each other, indicating the successful polymerization of acrylamide. The above two kinds of model microreactors based on the interfacial emulsification technique clearly show that it is a reliable droplet generation platform for chemical analysis and material synthesis. Notably, the interfacial emulsification device shares similar fluidic components and structure with glass capillary microfluidics. Therefore, this method might also be utilized to prepare heterogeneous droplets or particles, just like the glass capillary microfluidics was used to prepare Janus particles.[50]

4.4. Rapid MIC Tests of Infectious Bacterial Pathogens. The minimum inhibitory concentration (MIC), as a gold standard for evaluating the bacterial inhibition effect of antibiotics, plays a vital role in clinical therapy for bacterial infection[51] and new antibiotic discovery for superbugs.[52] Traditionally, as suggested and guided by the Clinical and Laboratory Standards Institute (CLSI), the most widely used MIC testing methods include the broth microdilution method and the agar plate dilution method. Recently, the droplet method for MIC testing[53−58] has attracted the interest of many chemists and biologists due to the advantages of low reagent consumption, massive repeats, and high sensitivity. However, the accessibility of droplet microfluidics is a limitation for many biological and clinical laboratories.

We applied the interfacial emulsification of multicomponent droplets for MIC testing. Two model microbes, including a Gram-positive strain (*S. aureus* ATCC 27217) and a Gram-negative strain (*E. coli* ATCC 25922), are selected for representative MIC measurements. Droplets quantitatively mixed with microbes and antibiotics were generated via the interfacial emulsification technique, and PMDAs were formed in a flat-bottomed 96-well plate (Figure 9a). The flow rates of each channel were tuned to achieve a concentration gradient of antibiotics among PMDAs in different wells. After incubation at 37 °C for 24 h, the plate was taken out for microscope inspection and the MIC value could be read on the basis of the turbidity difference between droplets with the help of an inverted microscope. As a result (Figure 9b−d), all of the droplets loaded with only *E. coli* ATCC 25922 and culture medium exhibit greater scattering of transmission light and appear dark gray with weak brightness, indicating that the bacteria grow well in the droplets (green dashed circle). As the concentration of antibiotic increases to a certain value, droplets tend to become more transparent with a brighter reflective surface (red dashed circle), referring to the fact that the bacterial growth is inhibited. As the concentration keeps increasing, all of the droplets eventually become bright and smooth. Herein, the growth percentage is defined as the percentage of gray droplets, representing the possibility of bacterial growth at a specific antibiotic concentration. The MIC value is defined as the concentration at which 99% of droplets become bright and clear, indicating a 99% possibility for successful bacterial inhibition at this concentration. As shown in Figure 10e,f, the MIC values of tetracycline with respect to *E. coli* ATCC 25922 and *S. aureus* ATCC 27217 are 1.56 and 1.71 μg/mL, respectively. The MIC results are consistent with MIC values tested by the traditional broth microdilution method (both 1 μg/mL), indicating that the interfacial emulsification technique is appropriate for droplet MIC testing.

DOI: 10.1021/acs.langmuir.8b01067
Langmuir XXXX, XXX, XXX−XXX

Besides the validation of MIC tests using model microbes, the above technique can be readily extended to clinical diagnosis as demonstrated by the antibiotic susceptibility testing of a clinical multidrug resistant strain, *K. pneumoniae* HS 11286.[59] With the same approach as stated above, the MIC values of levofloxacin and tetracycline with respect to this clinically isolated strain are determined (Figure 9g,h), which are consistent with the results obtained by the standard broth microdilution method (4 and 64 μg/mL). According to the Clinical & Laboratory Standards Institute (CLSI) criteria,[60] the MIC value of levofloxacin is approximately equal to the intermediate criteria from CLSI (4 μg/mL), indicating that *K. pneumoniae* HS 11286 is intermediate to levofloxacin. The MIC result of tetracycline is much higher than the criteria of CLSI (8 μg/mL), indicating that *K. pneumoniae* HS 11286 is resistant to tetracycline.

4.5. Preparation of Uniform Polymeric Microparticles Using Interfacial Emulsification. Polymeric microparticles for drug delivery have attracted tremendous attention in the past decade. The goal of polymeric microparticles for drug delivery is to release drugs in a predesigned location with a steady and controlled kinetic process. To achieve this goal, precise control over the particle size and uniformity is essential since a wide size distribution will lead to an uncontrollable initial burst release.[61,62] Precise control over the uniformity and composition of polymer particles will remarkably increase the repeatability and reliability. Hence, the selection of proper techniques for preparing polymeric microparticles has been taken into account. The microfluidics appears to be the most powerful tool for producing monodisperse droplets with a size ranging from several to hundreds of micrometers, affording great promise for the generation of polymeric microparticles with high uniformity. However, the serious deformation of elastomeric microchannels led by organic solvent is always raised on account of the swelling issue. This intrinsic incompatibility restricts the use of many θ solvents for dissolving particular polymers.

Interfacial emulsification is capable of generating highly uniform droplets with solvent-compatible fluidic channels, indicating that it can be a proper approach to the preparation of uniform polymeric microparticles. On the basis of the single-channel interfacial emulsification, chloroform dissolving a certain amount of polymer serves as the dispersed phase and 0.5 wt % sodium dodecyl sulfate aqueous solution is used as the continuous phase. For example, chloroform droplets loading different amounts of polystyrene were generated at a constant flow rate of 0.40 μL/min and a vibrational frequency of 50 Hz, and then chloroform was allowed to evaporate at 45 °C for several hours under mild shaking. Polymeric microparticles were yielded after being centrifuged from the continuous phase and washed with pure water to remove the surfactants. As shown in Figure 10a,b, uniform polystyrene microparticles with different sizes were prepared by utilizing the interfacial emulsification technique. As chloroform was evaporated, the droplet shrank and polystyrene was finally condensed into an object with a spherical shape. Thus, the size of polystyrene microparticles can be controlled by changing the polymer concentration in chloroform droplets. The results presented in Figure 10c are consistent with the predication, and the particle volume is nearly proportional to the polymer concentration. In addition to polystyrene microparticles, various kinds of uniform polymeric microparticles such as polylactic acid and polycarbonate can also be prepared via the interfacial emulsification technique.

To explore the full potential of interfacial emulsification in the preparation of polymeric microparticles, the interfacial emulsification technique can be combined with other fabrication approaches. Three kinds of polymer particles with irregular morphologies are exemplified, including elongated particles, particles with patchy surfaces, and porous particles (Figure 10d–f). Uniform elongated particles were obtained by stretching uniform spherical polycaprolactone particles that have been prepared via interfacial emulsification (Figure 10d). The preparation of patchy particles was based on the macroscopic phase separation between PS and PMMA. Droplets dissolving two free polymers of PS and PMMA are generated and solidified. Macroscopic phase separation between PS and PMMA drives one polymer to migrate onto the particle surface, although it has not been recognized which one is pushed out. Porous particles were synthesized via an in situ polymerization reaction within droplets. A photocurable monomer (trimethylolpropane triacrylate) with three methacrylate groups was loaded in droplets along with photoinitiator. Under UV irradiation, the droplet can be cross-linked into a gel together with solvents. The porous morphology is a result of the complete removal of solvents. All of these examples verify that the interfacial emulsification can serve as a versatile platform for the preparation of various kinds of polymeric microparticles.

5. CONCLUSIONS AND PERSPECTIVE

This feature article was focused on the interfacial emulsification technique that we developed over the past several years as an emerging droplet generation method. As stated, the droplet generation of interfacial emulsification mainly relies on an interfacial shearing process, and the droplet size is highly uniform and controllable. Interfacial emulsification has been successfully applied to the production of monodisperse droplets and microparticles, microreactors, and various kinds of bioanalysis. The advantages of interfacial emulsification are summarized as the following three points: (1) The fluidic channels of the interfacial emulsification platform can be made of materials that exhibit excellent compatible with various solvents, providing a versatile platform for droplet applications in chemical synthesis or reaction screening. (2) The whole device of the interfacial emulsification system is composed of low-cost components and can be modularly assembled within several minutes, ensuring that the method can be more available for researchers with different backgrounds. (3) The droplet volume can be easily calculated by dividing the flow rate by the vibrational frequency, and the droplet components can be simply predicted via a linear equation. The straightforward determination of droplet size and components makes it more accessible for users without any microfluidic experience.

However, as a newly developed technique, interfacial emulsification still has many critical shortcomings that need to be overcome for their future practical applications. Several issues are concerned: (1) The current method lacks the ability to manipulate and transfer droplets and to analyze single droplets. (2) The density of droplets must be higher than the continuous phase to allow the rapid sedimentation of generated droplets, and the smallest droplet volume is limited to tens of picoliters. (3) The interfacial vibrational process is restricted by manual adjustment of the distance between the capillary nozzle and the surface of continuous phase, and the resonance

DOI: 10.1021/acs.langmuir.8b01067
Langmuir XXXX, XXX, XXX−XXX

oscillation of the mechanical vibrator must be carefully investigated for reproducible droplet generation. (4) The maximum droplet generation efficiency of interfacial emulsification is about 500 droplets per second for one channel, which has lower throughput than chip-based droplet microfluidics. The poor throughput is the main circumstance for scalable material preparation, which may be overcome via parallel printing by using capillary arrays or utilizing devices with higher vibrational frequencies. (5) Extensive effort is still needed to integrate the interfacial emulsification technique with other automatic programs as an easy-to-use apparatus for various bioanalysis applications, such as the development of an automated and integrated digital PCR system. Although these challenges will not be fulfilled in the short term, we have solid confidence in the bright future of the interfacial emulsification technique. In future endeavors, the interfacial emulsification technique might play important roles in broader applications such as the controllable generation of complex emulsions, bacterial cell-cell interactions, and high-throughput assays of mammalian cells, organoids, or even whole animals such as *Caenorhabditis elegans*. With accumulated experience and continuous improvements to the interfacial emulsification technology, this emerging droplet generation platform will become an important supplement to current droplet microfluidics.

AUTHOR INFORMATION

Corresponding Authors

*E-mail: wenbin@im.ac.cn.
*E-mail: yapeiwang@ruc.edu.cn.

ORCID

Wenbin Du: 0000-0002-7401-1410
Yapei Wang: 0000-0001-5420-0364

Funding

This study was supported by the National Natural Science Foundation of China (21674127, 21422407, and 31470221), the National Key Research and Development Program of China (2016YFC0100900 and 2016YFE0205800), the Beijing Municipal Science & Technology Commission (Z161100000116042), the Chinese Academy of Sciences (XDB15040102, QYZDB-SSW-SMC008, and KFZD-SW-219-4), and the Open Research Fund of State Key Laboratory of Bioelectronics, Southeast University.

Notes

The authors declare no competing financial interest.

Biographies

Shenglong Liao received his B.E. and B.S. in materials chemistry and applied chemistry from the University of Science and Technology Beijing in 2015. He is currently a third-year graduate student under the supervision of Prof. Yapei Wang in the Department of Chemistry, Renmin University of China. He is pursuing research on the development of novel droplet generation methods and materials for microfluidic chip fabrication.

Yi Tao received her B.E. in biology from Northwest A&F University in 2015. She is currently a Ph.D. student at the Institute of Microbiology, Chinese Academy of Sciences under the supervision of Prof. Wenbin Du. She is dedicated to digital loop-mediated isothermal amplification research and its application in rapid quantitative detection and real-time monitoring of clinical pathogens.

Wenbin Du received his Ph.D. in chemistry from Zhejiang University in 2007. He was a postdoctoral researcher at the University of Chicago from 2007 to 2011. He joined the Institute of Microbiology, Chinese Academy of Sciences in 2013. His research laboratory specializes in microfluidics and microbiology applications.

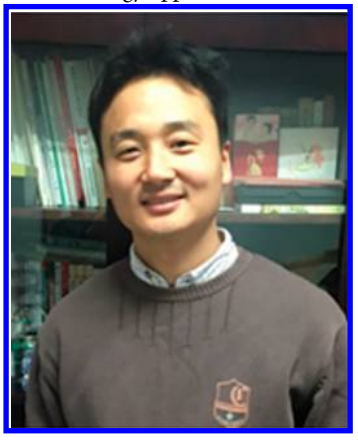

DOI: 10.1021/acs.langmuir.8b01067
Langmuir XXXX, XXX, XXX−XXX

Yapei Wang is a full professor in the Department of Chemistry, Renmin University of China. He received his B.S. from Jilin University in 2004 and Ph.D. from Tsinghua University under the supervision of Prof. Xi Zhang in 2009, both in chemistry. After graduation, he spent 2 years as a postdoctoral fellow in Prof. Joseph M. DeSimone's laboratory at the University of North Carolina at Chapel Hill. In 2012, he joined the Department of Chemistry, Renmin University of China. His research interests are mainly focused on photothermal conversion materials and their clinical applications.

■ ACKNOWLEDGMENTS

The authors thank Dr. Peng Xu for his help in revising this article and Xiao Liu for his help with the previous physical model.

■ REFERENCES

(1) Ennis, W. B., Jr.; James, D. T. A Simple Apparatus for Producing Droplets of Uniform Size from Small Volume of Liquids. *Science* **1950**, *112*, 434−436.
(2) Joensson, H. N.; Andersson, H. Droplet Microfluidics-A Tool for Single-Cell Analysis. *Angew. Chem., Int. Ed.* **2012**, *51*, 12176−12192.
(3) Baret, J.-C.; Miller, O. J.; Taly, V.; Ryckelynck, M.; El-Harrak, A.; Frenz, L.; Rick, C.; Samuels, M. L.; Hutchison, J. B.; Agresti, J. J.; Link, D. R.; Weitz, D. A.; Griffiths, A. D. Fluorescence-Activated Droplet Sorting (FADS): Efficient Microfluidic Cell Sorting Based on Enzymatic Activity. *Lab Chip* **2009**, *9*, 1850−1858.
(4) Elvira, K. S.; Casadevall i Solvas, X.; Wootton, R. C.; deMello, A. J. The Past, Present and Potential for Microfluidic Reactor Technology in Chemical Synthesis. *Nat. Chem.* **2013**, *5*, 905−915.
(5) Niu, G.; Ruditskiy, A.; Vara, M.; Xia, Y. Toward Continuous and Scalable Production of Colloidal Nanocrystals by Switching from Batch to Droplet Reactors. *Chem. Soc. Rev.* **2015**, *44*, 5806−5820.
(6) Parr, H. C. M.; Busvine, J. R. A Spinning-Disk Sprayer for Applying Residual Insecticides. *Ann. Appl. Biol.* **1948**, *35*, 359−368.
(7) Walton, W. H.; Prewett, W. C. The Production of Sprays and Mists of Uniform Drop Size by Means of Spinning Disc Type Sprayers. *Proc. Phys. Soc., London, Sect. B* **1949**, *62*, 341−350.
(8) Nakashima, T.; Shimizu, M.; Kukizaki, M. Particle Control of Emulsion by Membrane Emulsification and Its Applications. *Adv. Drug Delivery Rev.* **2000**, *45*, 47−56.
(9) Wang, R.; Zhang, Y.; Ma, G.; Su, Z. Preparation of Uniform Poly(glycidyl methacrylate) Porous Microspheres by Membrane Emulsification. *J. Appl. Polym. Sci.* **2006**, *102*, 5018−5027.
(10) Piacentini, E.; Drioli, E.; Giorno, L. Membrane Emulsification Technology: Twenty-Five Years of Inventions and Research through Patent Survey. *J. Membr. Sci.* **2014**, *468*, 410−422.
(11) Wang, Y.; Bokor, J.; Lee, A. Maskless Lithography Using Drop-on-Demand Inkjet Printing Method. *Proc. SPIE* **2004**, *5374*, 628−636.
(12) Staymates, M. E.; Fletcher, R.; Verkouteren, M.; Staymates, J. L.; Gillen, G. The Production of Monodisperse Explosive Particles with Piezo-Electric Inkjet Printing Technology. *Rev. Sci. Instrum.* **2015**, *86*, 125114.
(13) Udey, R. N.; Jones, A. D.; Farquar, G. R. Aerosol and Microparticle Generation Using A Commercial Inkjet Printer. *Aerosol Sci. Technol.* **2013**, *47*, 361.
(14) Anna, S. L.; Bontoux, N.; Stone, H. A. Formation of Dispersions Using "Flow Focusing" in Microchannels. *Appl. Phys. Lett.* **2003**, *82*, 364−366.
(15) Chu, L.; Utada, A. S.; Shah, R. K.; Kim, J.-W.; Weitz, D. A. Controllable Monodisperse Multiple Emulsions. *Angew. Chem., Int. Ed.* **2007**, *46*, 8970−8974.
(16) Thorsen, T.; Roberts, R. W.; Arnold, F. H.; Quake, S. R. Dynamic Pattern Formation in a Vesicle-Generating Microfluidic Device. *Phys. Rev. Lett.* **2001**, *86*, 4163−4166.
(17) Song, H.; Tice, J. D.; Ismagilov, R. F. A Microfluidic System for Controlling Reaction Networks in Time. *Angew. Chem., Int. Ed.* **2003**, *42*, 768−772.
(18) Cramer, C.; Fischer, P.; Windhab, E. J. Drop Formation in a Coflowing Ambient Fluid. *Chem. Eng. Sci.* **2004**, *59*, 3045−3058.
(19) Shang, L.; Cheng, Y.; Wang, J.; Ding, H.; Rong, F.; Zhao, Y.; Gu, Z. Double Emulsions from a Capillary Array Injection Microfluidic Device. *Lab Chip* **2014**, *14*, 3489−3493.
(20) Shang, L.; Cheng, Y.; Zhao, Y. Emerging Droplet Microfluidics. *Chem. Rev.* **2017**, *117*, 7964−8040.
(21) Whitesides, G. M. The Origins and The Future of Microfluidics. *Nature* **2006**, *442*, 368−373.
(22) Lee, J. N.; Park, C.; Whitesides, G. M. Solvent Compatibility of Poly(dimethylsiloxane)-Based Microfluidic Devices. *Anal. Chem.* **2003**, *75*, 6544−6554.
(23) Toepke, M. W.; Beebe, D. J. PDMS Absorption of Small Molecules and Consequences in Microfluidic Applications. *Lab Chip* **2006**, *6*, 1484−1486.
(24) Kaminski, T. S.; Scheler, O.; Garstecki, P. Droplet Microfluidics for Microbiology: Techniques, Applications and Challenges. *Lab Chip* **2016**, *16*, 2168−2187.
(25) Duncombe, T. A.; Tentori, A. M.; Herr, A. E. Microfluidics: Reframing Biological Enquiry. *Nat. Rev. Mol. Cell Biol.* **2015**, *16*, 554−567.
(26) Gu, H.; Duits, M. H.; Mugele, F. Droplets Formation and Merging in Two-Phase Flow Microfluidics. *Int. J. Mol. Sci.* **2011**, *12*, 2572−2597.
(27) Xu, P.; Zheng, X.; Tao, Y.; Du, W. Cross-Interface Emulsification for Generating Size-Tunable Droplets. *Anal. Chem.* **2016**, *88*, 3171−3177.
(28) Hu, Y.; Xu, P.; Luo, J.; He, H.; Du, W. Absolute Quantification of H5-Subtype Avian Influenza Viruses Using Droplet Digital Loop-Mediated Isothermal Amplification. *Anal. Chem.* **2017**, *89*, 745−750.
(29) Liao, S.; He, Y.; Wang, D.; Dong, L.; Du, W.; Wang, Y. Dynamic Interfacial Printing for Monodisperse Droplets and Polymeric Microparticles. *Adv. Mater. Technol.* **2016**, *1*, 1600021.
(30) Liao, S.; Tao, X.; Ju, Y.; Feng, J.; Du, W.; Wang, Y. Multichannel Dynamic Interfacial Printing: An Alternative Multicomponent Droplet Generation Technique for Lab in a Drop. *ACS Appl. Mater. Interfaces* **2017**, *9*, 43545−43552.
(31) Vogelstein, B.; Kinzler, K. W. Digital PCR. *Proc. Natl. Acad. Sci. U. S. A.* **1999**, *96*, 9236−9241.
(32) Hindson, B. J.; Ness, K. D.; Masquelier, D. A.; et al. High-Throughput Droplet Digital PCR System for Absolute Quantitation of DNA Copy Number. *Anal. Chem.* **2011**, *83*, 8604−8610.
(33) Men, Y.; Fu, Y.; Chen, Z.; Sims, P. A.; Greenleaf, W. J.; Huang, Y. Digital Polymerase Chain Reaction in an Array of Femtoliter Polydimethylsiloxane Microreactors. *Anal. Chem.* **2012**, *84*, 4262−4266.
(34) Chen, Z.; Liao, P.; Zhang, F.; Jiang, M.; Zhu, Y.; Huang, Y. Centrifugal Micro-channel Array Droplet Generation for Highly Parallel Digital PCR. *Lab Chip* **2017**, *17*, 235−240.
(35) Ottesen, E. A.; Hong, J. W.; Quake, S. R.; Leadbetter, J. R. Microfluidic Digital PCR Enables Multigene Analysis of Individual Environmental Bacteria. *Science* **2006**, *314*, 1464−1467.
(36) Baker, M. Digital PCR Hits Its Stride. *Nat. Methods* **2012**, *9*, 541−544.
(37) Heyries, K. A.; Tropini, C.; Vaninsberghe, M.; Doolin, C.; Petriv, O. I.; Singhal, A.; Leung, K.; Hughesman, C. B.; Hansen, C. L. Megapixel Digital PCR. *Nat. Methods* **2011**, *8*, 649−651.
(38) Sun, B.; Shen, F.; McCalla, S. E.; Kreutz, J. E.; Karymov, M. A.; Ismagilov, R. F. Mechanistic Evaluation of the Pros and Cons of Digital RT-LAMP for HIV-1 Viral Load Quantification on a Microfluidic Device and Improved Efficiency via a Two-Step Digital Protocol. *Anal. Chem.* **2013**, *85*, 1540−1546.
(39) Rane, T. D.; Chen, L.; Zec, H. C.; Wang, T. H. Microfluidic continuous flow digital loop-mediated isothermal amplification (LAMP). *Lab Chip* **2015**, *15*, 776−782.
(40) Shen, F.; Sun, B.; Kreutz, J. E.; Davydova, E. K.; Du, W.; Reddy, P. L.; Joseph, L. J.; Ismagilov, R. F. Multiplexed Quantification of Nucleic Acids with Large Dynamic Range Using Multivolume Digital

DOI: 10.1021/acs.langmuir.8b01067
Langmuir XXXX, XXX, XXX−XXX

RT-PCR on a Rotational SlipChip Tested with HIV and Hepatitis C Viral Load. *J. Am. Chem. Soc.* **2011**, *133*, 17705−17712.
(41) Kreutz, J. E.; Munson, T.; Huynh, T.; Shen, F.; Du, W.; Ismagilov, R. F. Theoretical Design and Analysis of Multivolume Digital Assays with Wide Dynamic Range Validated Experimentally with Microfluidic Digital PCR. *Anal. Chem.* **2011**, *83*, 8158−8168.
(42) Clementi, M. Quantitative Molecular Analysis of Virus Expression and Replication. *J. Clin. Microbiol.* **2000**, *38*, 2030−2036.
(43) *Manual for the Laboratory Diagnosis and Virological Surveillance of Influenza*; World Health Organization: Geneva, 2011.
(44) Harper, S. A.; Bradley, J. S.; Englund, J. A.; File, T. M.; Gravenstein, S.; Hayden, F. G.; McGeer, A. J.; Neuzil, K. M.; Pavia, A. T.; Tapper, M. L.; Uyeki, T. M.; Zimmerman, R. K. Seasonal Influenza in Adults and Children-Diagnosis, Treatment, Chemoprophylaxis, and Institutional Outbreak Management: Clinical Practice Guidelines of the Infectious Diseases Society of America. *Clin. Infect. Dis.* **2009**, *48*, 1003−1032.
(45) Song, H.; Tice, J. D.; Ismagilov, R. F. A Microfluidic System for Controlling Reaction Networks in Time. *Angew. Chem., Int. Ed.* **2003**, *42*, 768−772.
(46) Yin, S.-N.; Yang, S.; Wang, C.-F.; Chen, S. Magnetic-Directed Assembly from Janus Building Blocks to Multiplex Molecular-Analogue Photonic Crystal Structures. *J. Am. Chem. Soc.* **2016**, *138*, 566−573.
(47) Chan, E. M.; Alivisatos, A. P.; Mathies, R. A. High-Temperature Microfluidic Synthesis of CdSe Nanocrystals in Nanoliter Droplets. *J. Am. Chem. Soc.* **2005**, *127*, 13854−13861.
(48) Nightingale, A. M.; Phillips, T. W.; Bannock, J. H.; de Mello, J. C. Controlled Multistep Synthesis in A Three-Phase Droplet Reactor. *Nat. Commun.* **2014**, *5*, 3777.
(49) Yu, Z.; Zhang, J.; Coulston, R. J.; Parker, R. M.; Biedermann, F.; Liu, X.; Scherman, O. A.; Abell, C. Supramolecular Hydrogel Microcapsules via Cucurbit[8]uril Host-Guest Interactions with Triggered and UV-Controlled Molecular Permeability. *Chem. Sci.* **2015**, *6*, 4929−4933.
(50) Zhao, Y.; Gu, H.; Xie, Z.; Shum, H. C.; Wang, B.; Gu, Z. Bioinspired Multifunctional Janus Particles for Droplet Manipulation. *J. Am. Chem. Soc.* **2013**, *135*, 54−57.
(51) Andrews, J. M. Determination of Minimum Inhibitory Concentrations. *J. Antimicrob. Chemother.* **2001**, *48*, 5−16.
(52) O'Neill, A. J.; Chopra, I. Preclinical Evaluation of Novel Antibacterial Agents by Microbiological and Molecular Techniques. *Expert Opin. Invest. Drugs* **2004**, *13*, 1045−1063.
(53) Boedicker, J. Q.; Li, L.; Kline, T. R.; Ismagilov, R. F. Detecting Bacteria and Determining Their Susceptibility to Antibiotics by Stochastic Confinement in Nanoliter Droplets Using Plug-Based Microfluidics. *Lab Chip* **2008**, *8*, 1265−1272.
(54) Churski, K.; Kaminski, T. S.; Jakiela, S.; Kamysz, W.; Baranska-Rybak, W.; Weibel, D. B.; Garstecki, P. Rapid Screening of Antibiotic Toxicity in an Automated Microdroplet System. *Lab Chip* **2012**, *12*, 1629−1637.
(55) Cao, J.; Kürsten, D.; Schneider, S.; Knauer, A.; Günther, P. M.; Köhler, J. M. Uncovering Toxicological Complexity by Multi-Dimensional Screenings in Microsegented Flow: Modulation of Antibiotic Interference by Nanoparticles. *Lab Chip* **2012**, *12*, 474−484.
(56) Baraban, L.; Bertholle, F.; Salverda, M. L.; Bremond, N.; Panizza, P.; Baudry, J.; de Visser, J. A. G. M.; Bibette, J. Millifluidic Droplet Analyser for Microbiology. *Lab Chip* **2011**, *11*, 4057−4062.
(57) Kaminski, T. S.; Scheler, O.; Garstecki, P. Droplet Microfluidics for Microbiology: Techniques, Applications and Challenges. *Lab Chip* **2016**, *16*, 2168−2187.
(58) Liu, X.; Painter, R. E.; Enesa, K.; Holmes, D.; Whyte, G.; Garlisi, C. G.; Monsma, F. J., Jr.; Rehak, M.; Craig, F. F.; Smith, C. A. High-Throughput Screening of Antibiotic-Resistant Bacteria in Picodroplets. *Lab Chip* **2016**, *16*, 1636−1643.
(59) Liu, P.; Li, P.; Jiang, X.; Bi, D.; Xie, Y.; Tai, C.; Deng, Z.; Rajakumar, K.; Ou, H.-Y. Complete Genome Sequence of Klebsiella pneumoniae subsp. pneumoniae HS11286, a Multidrug-Resistant Strain Isolated from Human Sputum. *J. Bacteriol.* **2012**, *194*, 1841−1842.
(60) *Clinical and Laboratory Standards Institute. Performance Standards for Antimicrobial Susceptibility Testing*; Twenty-Fifth Informational Supplement; www.clsi.org, 2015.
(61) Kost, J.; Langer, R. Responsive Polymeric Delivery Systems. *Adv. Drug Delivery Rev.* **2001**, *46*, 125−148.
(62) Xu, Q.; Hashimoto, M.; Dang, T. T.; Hoare, T.; Kohane, D. S.; Whitesides, G. W.; Langer, R.; Anderson, D. G. Preparation of Monodisperse Biodegradable Polymer Microparticles Using a Microfluidic Flow-Focusing Device for Controlled Drug Delivery. *Small* **2009**, *5*, 1575−1581.

DOI: 10.1021/acs.langmuir.8b01067
Langmuir XXXX, XXX, XXX−XXX